

2-2-7 Long-term Forecast of the Occurrence Probabilities of Intense Geomagnetic Storms

TSUBOUCHI Ken

Long-term forecast of the occurrence probabilities of intense geomagnetic storms is quantitatively given by analyzing the statistics of the Dst-index time-series database from 1957 to 2001. The main purpose was to derive two parameters acting as proxies for the long-term (monthly to yearly scale) features of storms, the probable intensity and the occurrence frequency within the unit period. The probable intensity represents the expected maximum storm level with an occurrence rate of once per T -years, which is given as a function of T and is derived by applying the extreme value theory to the extreme Dst data subset. The occurrence probability is evaluated under the assumption that the storm occurrence follows the Poisson process, where the average occurrence rate is different between active and quiet period in a solar cycle.

Keywords

Geomagnetic storms, Occurrence probabilities, Long-term forecast, Extreme value statistics, Poisson distribution

1 Introduction

Space activities in contemporary society have rising value as a social infrastructure in the form of manned activities related to artificial satellites used in communications, broadcasts, observations, and other operations, along with the practical use of outer space. However, the environment for such activities is severe due to constant exposure to energetic particles, anomalous currents, and similar factors. Phenomena discovered conventionally in satellite observation and similar activities are regarded as real “natural disasters and risks”. An anomalous increase in energetic particle flux, for example, causes electronic circuit damage and communication disorders in artificial satellites, increases the possibility of exposure among astronauts, aircraft crews, and other personnel, and results in the formation of a current system known to induce breakdowns in aboveground power transmission systems. Solar flares, coronal mass ejection (CME), and other explosive

solar phenomena are particularly notable in that all have often caused catastrophic damage to satellites and other facilities. Today, the National Institute of Information and Communications Technology (NICT) mainly promotes “space weather forecast” by conducting analysis taking full advantage of simulations based on a wide-ranging observation network extending from the ground to outer space and utilizing a leading-edge supercomputer to predict the occurrence of such risk phenomena, thereby stably promoting the future use of outer space. One main activity is the short-term prediction of phenomena induced by activity observed on the solar surface with a leading time of daily range before such phenomena reaches the earth’s magnetosphere. On a practical level, conceivable applications include the issuing of real-time warnings when an explosive solar phenomenon is detected such as through satellite operation. Here, predictions of the time it will take for a disaster phenomenon to arrive and its intensity represent the information

required on a practical level. On the other hand, a quantitative evaluation of risks due to an activity spanning a long period (of several months to several years) will become important in estimating projected loss and other aspects of operation. The information required in such a case includes the maximum intensity and frequency of disaster phenomena during the activity period. At the moment, few studies focus on “long-term predictions” based on statistics of time series data compared with “short-term predictions” based on the demand of the physical cause-and-effect principle. In this paper, a time series database is used to introduce probability values that quantifying the occurrence probability of risk events, where focus is placed on the statistical nature of “extreme data,” well beyond the long-term average as well as its normal noise. A study will be conducted on specific examples of long-term predictions of space weather based on studies detailed in Reference [1] that focus particularly on geomagnetic storm events.

2 Discussion

2.1 Geomagnetic storms

This paper discusses geomagnetic storm events as “natural risk phenomena” of outer space that are most important in the environment surrounding the earth and which exercise various influences on our space activities. The main factor of geomagnetic storms is the interaction between a southward interplanetary magnetic field (IMF) and the earth’s magnetosphere over a long period accompanied by coronal mass ejection (CME) and other phenomena released by the sun, thereby causing large quantities of solar wind plasma entering the magnetosphere to form a large current structure such as the equatorial ring current (see Reference [2]). The Dst index expresses the magnitude of geomagnetic storms, that is, the magnitude of geomagnetic disturbances observed at geomagnetic observatories (at four widespread locations in terms of longitude) in the mid-

latitudes as expressed as an index of one-hour average values, and mainly represents the intensity of equatorial ring current. In the presence of a geomagnetic storm, a strong westward equatorial ring current is generated, thereby inducing a southward magnetic field on the ground. As a result, the Dst index declines quickly (several hours to about one day) and then gradually recovers to a normal-state level. The present study used a data set containing 45 years’ worth of data from 1957 to 2001 (provided by Kyoto University’s World Data Center for Geomagnetism, and including a total of 394,464 items of data). As an example, Fig. 1 shows a time series plot of Dst indexes during the year 2000. The basic statistic of the Dst index during that year is -20 nT on average, with deviation of about 28 nT and skewness of about -3 . While small-scale random changes are indicated under normal states, the presence of a major geomagnetic storm event suddenly developing in the negative direction proves that the distribution of the Dst index is distorted in the negative direction. Geomagnetic storms are classified into three categories (intense, moderate or small) according to the minimum value when the Dst index is at its peak [2]. Of particular interest is that an intense event ($Dst < -100$ nT) is known to occur when the (IMF) remains southward for more than three hours, resulting in a remark-

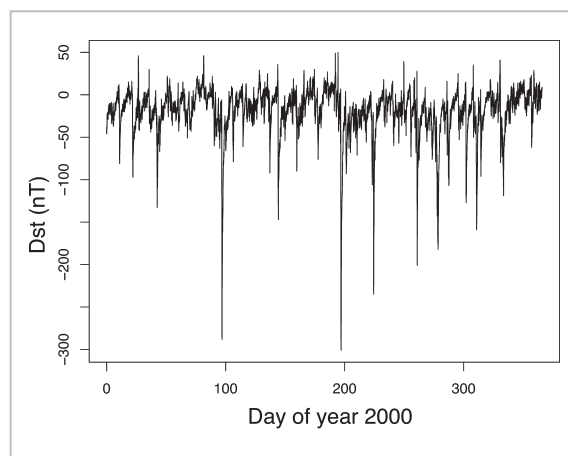


Fig. 1 Time series plot of Dst indexes (with the x-axis representing the day of the year) for the year 2000

able rise in the high-energy particle flux of auroral activity and the radiation belt.

In this paper, geomagnetic storm events are defined by the Dst data subset where Dst successively remains less than -100 nT. To assure an independent feature among each event, the events with intervals of less than 48 hours are regarded as being identical. Consequently, a total of 322 events were extracted during the 45 years from 1957 to 2001. This means that one such event occurred every 1.7 months on average. Here, Fig. 2 is a scatter plot between the two parameters: the intensities of geomagnetic storms defined by the minimum Dst per event (I_s), and the intervals between neighboring events at their Dst peak time (T_s). An inverse proportionate trend between I_s and T_s is also evident in Fig. 2 as a tendency where, the stronger the magnetic storm, the shorter the interval from the last event. Of particular interest is a huge event where $I_s < -280$ nT, suggesting a relatively moderate magnitude of an event that occurred during the previous six months (up to 5,000 hours), and such event can possibly be regarded as a precursor phenomenon in long-term prediction. Moreover, this trend is presumably closely related to the accumulation and release processes of energy in the magnetosphere, although subsequent analysis and discussion exceed the scope of this paper. The following section regards the maximum possible intensities and occurrence frequency on monthly and yearly levels as basic parameters for these intense events, and validates the probability of occurrence.

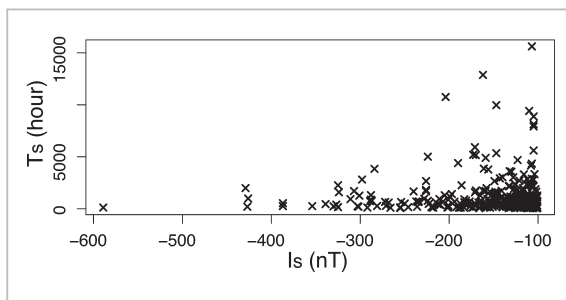


Fig.2 Correlation between the intensity (I_s) and interval (T_s) of geomagnetic storm events

2.2 Maximum intensity

This section discusses statistical estimates of the maximum intensity of geomagnetic storms projected to occur in the future. When considering the risks to space activities, the frequency of such storms occurring may be extremely low, but the occurrence of any such major event is likely to cause a fatal disorder. To avoid such risks and minimize resulting losses, it is important to make appropriate quantitative estimates of the maximum generable scale of such event levels in the future without any particular underestimation or overestimation involved.

First of all, Fig. 3 shows the general distribution of $Dst < -10$ nT. The intense event ($Dst < -100$ nT) discussed in this paper corresponds to the right tail of this distribution and occurs with a frequency of about 1% (4632) among all the data items (394,464). From this figure, one can see that the tail shows a power-law distribution, so that the standard quantities such as the average or deviation are not suitable for describing the statistical features in this part. Moreover, assuming a normal distribution will result in underestimating the occurrence frequency of events. Therefore, another statistical method

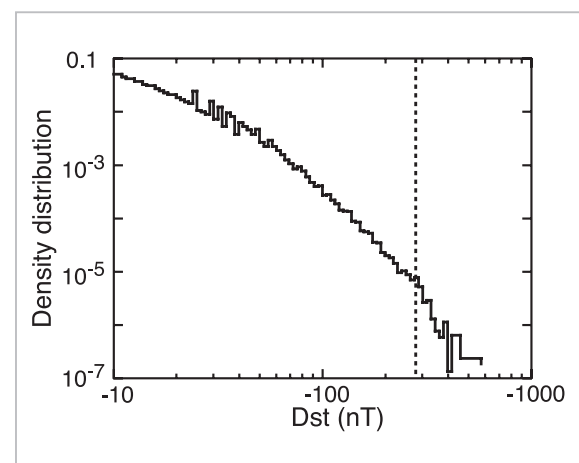


Fig.3 Density distribution function of the Dst index (with display limited to -10 nT or less and both coordinates being a plot of logarithms)

The analysis of extreme value statistics as discussed in this paper only extracted the data of $Dst < -280$ nT (portion to the right of the dotted line).

must be introduced with regard to risk management against disasters.

This paper thus attempts to use extreme value statistics (see References [3] and [4]). Extreme value statistics are intended for use in discussing such matters as the distribution shape designed specifically for the tail portion for data indicating target phenomena, eliminating the “normal state” effects accounting for a majority of the data, and enabling the highly precise statistical analysis of risky events. Civil engineering and risk finance are among the typical areas of application thus far. For example, people suffered great damage due to a major flood that occurred in the Netherlands in the 1950s, and this method was used for designing embankments at appropriate heights to ensure long-term safety in land areas below sea level. (In this example, calculations were made for the height at which seawater would overrun the embankments with a probability of about once every 10,000 years.) Extreme value statistics were applied in order to examine the statistics of extremely major events in the Ap index, proton flux of 60 MeV or more as observed by IMP satellites, and electron flux of 2 MeV or more as observed by GOES satellites [5]. In recent years, extreme value statistics have also been used to estimate the upper limit value of MeV electron flux in the outer radiation belt [6]. The present study employed this method for the Dst index to derive the distribution function of extreme Dst, which leads to a quantitative estimate of the maximum intensity of magnetic storms projected to occur in the future (several years to tens of years) as a function of the estimation period.

Extreme value statistics are based on a predetermined form of the (cumulative) probability distribution function for the extreme data being handled. Given the nature of the data set used, the functions are classified into two main categories: (1) generalized extreme value (GEV) distribution based on documents of maximum values, and (2) generalized Pareto distribution (GPD) based on doc-

uments of threshold exceedances. Categories (1) and (2) use different methods of extracting data sets designed specifically for extreme value statistics from all data items. Category (1) divides the whole data set for each period (such as one year) and composes subsets of maximum values only during each period. Conversely, category (2) sets a certain threshold and composes subsets that only extract data exceeding that threshold. Giving the data value as x yields GEV and GPD as follows:

$$\text{GEV: } G_{\gamma}(x) = \exp(-(1 + \gamma x)^{-1/\gamma})$$

$$\text{GPD: } W_{\gamma}(x) = 1 - (1 + \gamma x)^{-1/\gamma}$$

Here, γ is called the shape parameter of distribution. Moreover, replacing x with $(x - \mu) / \sigma$ (with μ denoting the location parameter and σ the scale parameter) enables the handling of a desired item of extreme value data. Location parameter μ represents the threshold that characterizes extreme value data.

Here, the author intended to extract the Dst index data exceeding threshold μ and fit the generalized Pareto distribution of (2), thereby estimating each parameter, γ and σ . (However, the argument of the distribution function is defined with a positive value, so that data is given as |Dst|.) Extreme value statistics hold that all data exceeding threshold μ should follow the same distribution. Figure 3 shows that a distribution of Dst < -280 nT can be approximated using the same power-law distribution (with its index of up to -4.96); therefore, this paper proceeds with calculations based on $\mu = 280$. There are a total of 121 documents of exceedances satisfying this condition, meaning that this condition occurs 2.7 times a year on average. The maximum likelihood method was used for estimating parameters. (The tool actually used was the extreme value statistics analysis package (extRemes) for statistical analysis software R.) The most likely solution given from the fitting result of $(\mu, \gamma, \sigma) = (280,$

0.177 ± 0.117 , 38.2 ± 5.6) was used to take |Dst| on the x-axis, cumulative probability on the y-axis, and a plot based on $W_{\mu, \gamma, \sigma}(|Dst|) = 1 - (1 + \gamma(|Dst| - \mu)/\sigma)^{-1/\gamma}$ (Fig. 4). Here, we can see that the mark x represents a real Dst value, which agrees well with the form of function obtained.

Based on this Pareto distribution, an important quantity called the T -year return level (S_T) is determined. This represents the maximum intensity that may occur during a determined period (of T years) in the future and is defined from a point where an event exceeding S_T will occur with a probability of once every T years. The final objective of this section is to determine S_T as a function of said T years.

The following briefly summarizes how S_T is derived. First, the total number of Dst data items obtained in T years is $N_T = 365.25 \times 24 \times T$ and, from the definition of S_T , the result is $\Pr\{X \geq S_T\} = 1/N_T$. Based on the principle that generalized Pareto distribution $W_{\mu, \gamma, \sigma}(x) = 1 - (1 + \gamma(x - \mu)/\sigma)^{-1/\gamma}$ is cumulative probability $\Pr\{X < x | X > \mu\} = 1 - \Pr\{X \geq x | X > \mu\}$, this can be rewritten as $\Pr\{X > S_T\} = \Pr\{X > \mu\} \cdot \Pr\{X \geq S_T | X > \mu\} = \Pr\{X > \mu\} \{1 - W_{\mu, \gamma, \sigma}(S_T)\}$. Among the total number of data items (n), let the number of data items exceeding threshold μ be k (and approximated as $\Pr\{X > \mu\} = k/n$), and thus organizing the above will produce the T -year return level as given in the following equation:

$$S_T = \mu + \frac{\sigma}{\gamma} \left\{ \left(\frac{N_T k}{n} \right)^\gamma - 1 \right\}$$

Using this result enables an estimation of Dst values when a geomagnetic storm occurs regarding whether it is “the biggest in 10 years,” “the biggest in 50 years,” or “the biggest in 100 years,” respectively, as $(S_{10}, S_{50}, S_{100}) = (-450.8 \text{ nT}, -578.2 \text{ nT}, -645.3 \text{ nT})$. Figure 5 is a plot of S_T (solid lines) as a function of T years and the 95% confidence interval (broken lines). (For details on the calculation of standard deviation, see References [1] and [3].) The black dots are based on the intensity (I_s) value from the geomagnetic storm event (minimum Dst < -100 nT, 322 events) extracted in the preceding section. More specifically, the calculations were performed as described below. Let the number of events more intense than a certain I_s value be m , with an occurrence probability of once every 45/ m years, as plotted based on $S_T = I_s$ and $T = 45/m$ in Fig. 5. This figure shows that when $T = 10$ years or less, S_T is overestimated (with the actual estimate not reflected during quiet periods of solar activity) and that, with a span of more than 10 years, the evaluation is appropriate. This suggests that the method described in this section is effective in estimating maximum intensity during a period lasting longer than

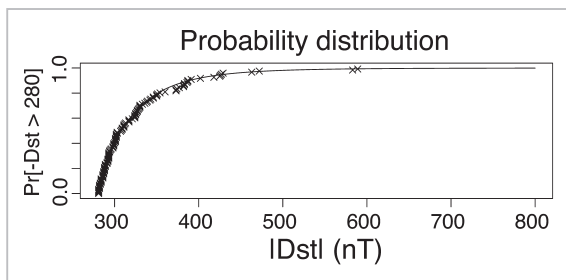


Fig.4 Generalized Pareto distribution function $W_{\mu, \gamma, \sigma}(|Dst|)$ as the result of fitting with Dst < -280 nT data

Note that $\mu = 280$, $\gamma = 0.177$ and $\sigma = 38.2$ were substituted. The mark x denotes the sorted Dst data used for fitting in sequence.

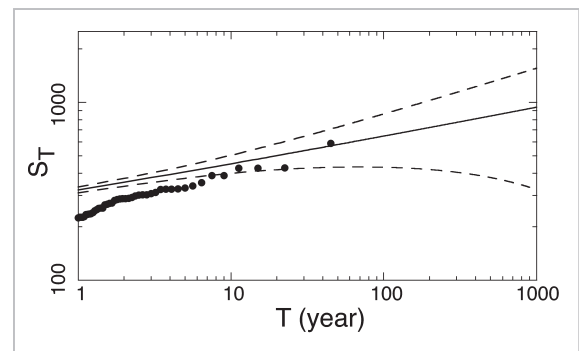


Fig.5 Plot of the T -year return level (solid line). The broken line represents the 95% confidence interval. The black dots represent the return level based on the actual intense event set.

the solar cycle.

2.3 Occurrence frequency

When making a prediction of event occurrences on the temporal axis, it is important in short-term prediction to make an accurate determination by pinpointing the time when a risk event will occur, where the main forecast tool is numerical simulation based on solar activity and solar wind data as input parameters. In contrast, in long-term prediction, the occurrence frequency over a span of several months to several years rather than accurate prediction of the occurrence time is even more essential information. This section extracts specific geomagnetic storm events, validates the statistical nature of that time series of occurrence, and provides probabilities regarding the predicted occurrence frequency of geomagnetic storms, such as the percentage of such events that will occur at least twice during the next six months.

The intense event considered here is such that the number of observation samples is very small compared with its percentage among all the data items, so that the occurrence process on the time series is projected to be approximated as a Poisson process. In the Poisson process, the interval (waiting time) between events follows exponential distribution $\lambda \exp(-\lambda t)$. The distribution of parameter T_s introduced in Section 2.1 is of the power-law type ($T_s^{-\alpha}$: with power index α of up to -2.06) at the tail of $T_s > 1,000$ hours. Although at a glance this may appear to be contradictory with the assumption of the Poisson process, Reference [7] describes the analysis of a similar distribution of the occurrence interval of solar flares that found parameter λ of the Poisson process to be time-dependent and that, if its distribution is of the power-law type, the occurrence interval would also be distributed in a power-law type as well. This analysis derived the power-law index of distribution α as being up to -2.2 ± 0.1 , thereby showing general agreement with the power-law index in the distribution of the magnetic storm interval (T_s) ana-

lyzed in this paper. However, discussing the correlation between magnetic storms and solar activity based on this fact alone constitutes a matter lacking sufficient material, and thus exceeds the scope of this paper.

The occurrence frequency actually depends largely on the degree of solar activity, and thus cannot be described with the same Poisson process throughout the period. Figure 6 shows the cumulative count in the order of occurrence of geomagnetic storm events extracted in Section 2.1 (black dots). The solid line represents the corresponding sunspot number as a monthly average. The inclination of the cumulative count in this plot indicates the average occurrence frequency, but Fig. 6 clearly shows that the inclination is not constant and exhibits zigzag changes that can be approximated locally as a straight line according to the solar activity phase (active and quiet). Moreover, one can see zigzag bends occurring around the border close to the point with a sunspot number of about 40, and that the period of such changes agrees well with the 11-year period of solar cycle (see the horizontal broken line in the

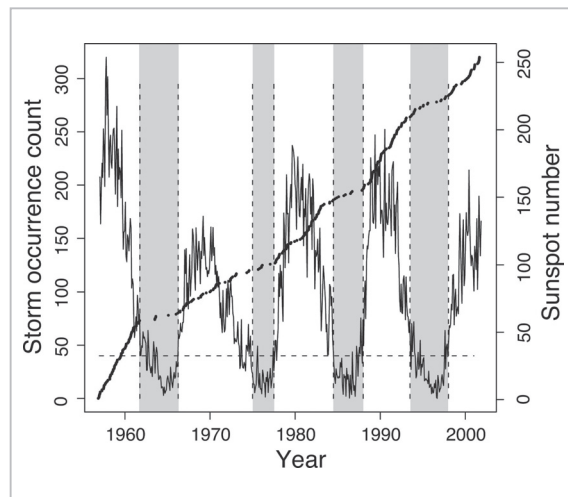


Fig. 6 Cumulative count (dots) regarding the occurrence of intense geomagnetic storm events. The solid line represents the sunspot number as a monthly average.

A quiet solar period is defined by the gray-shaded period. [The border is when the sunspot number is 40 (and indicated by a horizontal broken line).]

middle portion of Fig. 6). With this sunspot number of 40 as a point of division, the entire period of solar activity is divided into a quiet period and an active period (with the section shaded gray being the quiet period in Fig. 6).

Assuming that specific geomagnetic storms occur independently of one another, their occurrence process can be considered Poisson process $X(t)$. Letting the frequency of events (occurrence frequency) per unit period be λ , the probability distribution of frequency $X(t)$ of events in the time interval $[0, t]$ follows the Poisson distribution.

$$\Pr\{X(t) = k\} = (\lambda t)^k \exp(-\lambda t) / k!$$

Since the Poisson distribution is expected to become $E[X(t)] = \lambda t$, the inclination of the cumulative count in Fig. 6 will correspond to λ . The author then determined the inclination of a straight line in each phase (quiet and active periods). The result was that, when the unit period was three months, the average frequency of geomagnetic storms was about 0.7 times during the quiet period, and about 2.3 times during the active period. Preparing the distribution of the occurrence frequency of actual geomagnetic storms every three

months and examining its correspondence to the Poisson distribution revealed similar results, and thus the null hypothesis regarding the proposition that “the occurrence of geomagnetic storms follows the Poisson process in the quiet and active periods of solar activity” was rejected. Figure 7 is a plot of the probability distribution regarding the occurrence frequency every three months. The solid line represents the Poisson distribution during the active period ($\lambda = 2.3$), and the broken line represents that during the quiet period ($\lambda = 0.7$). The close and open circles respectively represent the actual frequency of each, and from this figure we can also see that approximation based on the Poisson process is appropriate.

Figure 8 shows the relation between parameter λ of the Poisson distribution during each active period and the maximum sunspot number during the corresponding solar cycle. The figure indicates that an almost linear relation exists between said parameter and sunspot number. This may suggest that the maximum sunspot number represents the degree of activity in the entire solar cycle, thereby positively affecting the occurrence frequency of geomagnetic storms, though

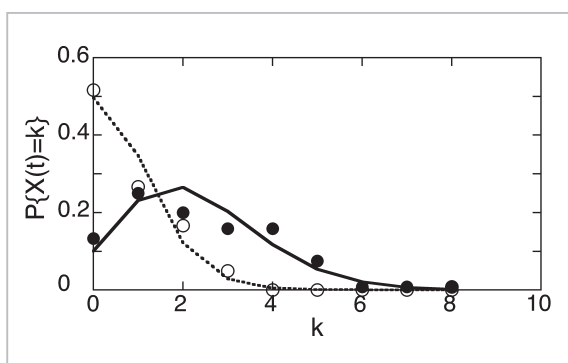


Fig.7 Distribution of probabilities for an intense geomagnetic storm event occurring k times every 3 months

The solid and broken lines represent the Poisson distribution in the solar active and quiet period, respectively. [Parameter $\lambda = 2.3$ (active period) or $= 0.7$ (quiet period)]. The close and open circles represent the actual distribution of occurrence frequencies at which they occurred during the active and quiet periods, respectively.

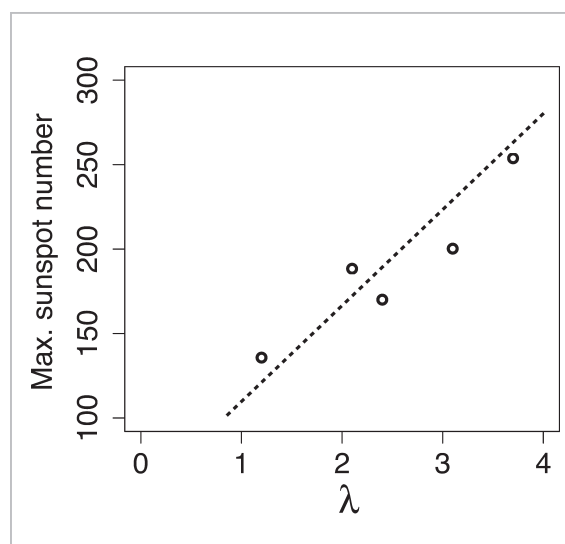


Fig.8 Correlation between the parameter of Poisson distribution during the solar active period (of 3 months) and the maximum sunspot number

this topic needs more elaborate verification in the future. Moreover, since the governing prediction when this relation holds true is that the maximum sunspot number in the next cycle (24) will become lower (see Reference [8]), the occurrence of intense geomagnetic storm events is expected to decline as well. For this topic, the author intends to further compare and verify the results obtained in the next actual period cycle.

Using the results above (estimation of parameter λ) enables a long-term forecast as described below. **“The probability is **% that an intense geomagnetic storm event will occur three or more times during the next three months”.**

This probability can be given by:

$$\begin{aligned} \Pr\{X(t) \geq 3\} &= 1 - \Pr\{X(t) < 3\} \\ &= 1 - \sum_{i=0}^2 \lambda^i \exp(-\lambda) / i! \end{aligned}$$

During the active period, the probability can be estimated at about 40% by using $\lambda = 2.3$. Such a probability generally has low scientific value (in that things with scientific significance only take values of 0 or 1 in terms of probability). At a practical level on the other hand, when the kind of damage that will occur in one event in a certain space activity is known, this method can be expected to be used in posting the expectation of total damage during a long-term operation. Moreover, based on this result, this method can also be applied to the development of insurance products and for similar purposes.

3 Conclusion

This paper focused on evaluating the occurrence of unavoidable natural risks in conducting space activities, particularly as a probability over a long period (in years). The author used intense geomagnetic storm events as a specific phenomenon, introduced an analysis method concerning the maximum intensity and frequency expected to occur in the future, and quantified the probability by

using a data set of 45 years' worth of the Dst indexes for magnetic storms. Maximum intensity was estimated by applying the statistics of rarely observed “extreme phenomena” to the Dst data set, in order to establish a procedure for determining the intensity with which such phenomena occur with a probability of once every T years in the future (T -year return level). Moreover, based on the precondition that specific magnetic storms occur independently, the Poisson process was used to propose a scheme for deriving the probability of future occurrence frequency.

While real-time prediction in units of hours to days is the mainstream in today's space weather studies, this paper focused on evaluating probability in consideration of practical use, particularly for predicting long-term risks on a monthly to yearly basis based on the statistics of events. Conversely, one could also say that the parameters determined here include information about critical phenomena in the solar-terrestrial system in the process of accumulating energy—topics that the author may incorporate in the future as an area of purely scientific research.

In order to make long-term forecasts even more precise, the analysis method introduced in this paper must also be further improved. For example, parameter λ in the Poisson distribution assumed in predicting the occurrence frequency of geomagnetic storms, was only given in two categories (i.e., quiet and active periods of solar cycle), but this is actually a very rough classification. For the occurrence frequency of solar flares, Reference [7] employs a method based on Bayes' statistics to determine the temporal changes in λ with even higher precision. Since there are overwhelmingly fewer geomagnetic storm events that occur than solar flares, one cannot say that the method mentioned above is necessarily suitable. However, for geomagnetic storms, the author wishes to adopt Bayes' statistics, the Kalman filter technique, and other statistical methods to derive parameters based more on real time.

In considering the practical aspects of

space weather forecasts, there are certain added limitations, such as the chaotic behavior caused by very small disturbances, the quality of data used, and the time required until a forecast can be provided. We can therefore say that a 100% accurate forecast is virtually impossible. In actual operation, the general agreement between a predicted probability and actual probability will be regarded

as more important than the physical correlation. It is therefore necessary to develop a method of quantitatively evaluating the cost and loss stemming from operation or non-operation based on a specific forecast.

The author wishes to acknowledge Kyoto University's World Data Center for Geomagnetism for its kind permission to use the database of Dst indexes in this study.

References

- 1 Tsubouchi, K. and Y. Omura, "Long-term occurrence probabilities of intense geomagnetic storm events," *Space Weather*, Vol. 5, S12003, doi: 10.1029/2007SW000329, 2007.
- 2 Gonzalez, W. D., J. A. Joselyn, Y. Kamide, H. W. Kroehl, G. Rostoker, B. T. Tsurutani, and V. M. Vasylunas, "What is a geomagnetic storm?," *J. Geophys. Res.* Vol. 99, No. A4, pp. 5771–5792, 1994.
- 3 Coles, S., "An Introduction to Statistical Modeling of Extreme Values," Springer, London, 2001.
- 4 Reiss, R.-D. and M. Thomas, "Statistical Analysis of Extreme Values," Birkhauser, Boston, 2001.
- 5 Koons, H. C., "Statistical analysis of extreme values in space science," *J. Geophys. Res.*, Vol. 106, No. A6, pp. 10915–10921, 2001.
- 6 O'Brien, T. P., J. F. Fennell, J. L. Roeder, and G. D. Reeves, "Extreme electron fluxes in the outer zone," *Space Weather*, Vol. 5, S01001, doi: 10.1029/2006SW000240, 2007.
- 7 Wheatland, M. S. and Y. E. Litvinenko, "Understanding solar flare waiting-time distributions," *Solar Physics*, Vol. 211, pp. 255–274, 2002.
- 8 Watari, S., "Forecasting solar cycle 24 using the relationship between cycle length and maximum sunspot number," *Space Weather*, Vol. 6, S12003, doi: 10.1029/2008SW000397, 2008.



TSUBOUCHI Ken, Ph.D.

*Expert Researcher, Space Environment
Group, Applied Electromagnetic
Research Center
Space plasma physics*